Appl. Phys. B 88, 221–226 (2007)
DOI: 10.1007/s00340-007-2682-y

**Applied Physics B**
**Lasers and Optics**

S.T. LI
X.Y. ZHANG✉
Q.P. WANG
P. LI
J. CHANG
X.L. ZHANG
Z.H. CONG

# Modeling of Q-switched lasers with top-hat pump beam distribution

School of Information Science and Engineering, Shandong University, Jinan, 250100, P.R. China

**Received: 22 February 2007 / Revised version: 1 May 2007**
**Published online: 15 June 2007 •** 

**ABSTRACT** For laser diode end-pumped solid-state lasers, the pump beam can be considered to be a Gaussian distribution or a top-hat distribution or between them. The rate equations for Q-switched lasers have been treated before, by considering the pump beam as a Gaussian distribution. This paper deals with the rate equations and the solutions for Q-switched lasers under a top-hat pump beam distribution. The normalized rate equation is obtained and solved numerically. A group of general curves are given and the comparison with the results under the Gaussian pump beam distribution and the plane-wave approximation is made. The results show that the solutions of the rate equations under a top-hat pump beam distribution are different from those under a Gaussian pump beam distribution, but the difference is very small. The solutions of the rate equations under both situations can give much more precise theoretical results than those under the plane-wave approximation.

**PACS** 42.60.Gd; 42.55.Xi; 42.55.Ah

## 1 Introduction

Q-switched lasers are efficacious tools to generate nanosecond and subnanosecond high-power giant pulses. Q-switched lasers include actively Q-switched lasers and passively Q-switched lasers. Actively Q-switched lasers with electro-optic modulators or acousto-optic modulators are more stable and controllable, while passively Q-switched lasers with saturable absorbers are more compact.

The standard tools for analyzing the performance of a Q-switched laser are the rate equations. For actively Q-switched lasers, the rate equations under the plane-wave approximation were first given by Wagner and Kay [1, 2]. These rate equations have been widely referred to and appropriately modified to make them more precise [3–9]. The dependences of the laser pulse characteristics on the finite lower laser level lifetime [3–5], laser energy level manifolds [6] and the thermalization time between levels in one manifold [7] were analyzed successively. An optimization analysis was made [8, 9]. Later, in 1999, the spatial variation of pumping and intracavity photon density in the rate equations was taken into account [10]; these space-dependent rate equations are particularly necessary for laser diode (LD)-pumped Q-switched lasers. For passively Q-switched lasers, the rate equations under the plane-wave approximation were first given by Szabo et al. [11–13]; these rate equations have undergone a similar process of modification to make them more precise [14–21].

For laser diode end-pumped solid-state lasers, the pump beam can be considered to be a Gaussian distribution in some situations and a top-hat distribution in some other situations. Sometimes the pump beam distribution is between the above two situations. The rate equations for passively Q-switched lasers have been treated by considering the pump beam as a Gaussian distribution [21]. This paper will focus on the rate equations and solutions for Q-switched lasers under a top-hat pump beam distribution. Because the theoretical description of an actively Q-switched laser can be considered as one special situation of a passively Q-switched laser in which the saturable absorber is extremely easy to be bleached [22], we only treat passively Q-switched lasers in this paper.

## 2 Rate equations

The rate equations including the transverse distribution describing passively Q-switched lasers can be written as [21]

$$\int_0^\infty \frac{\mathrm{d}\varphi(r,t)}{\mathrm{d}t} 2\pi r\,\mathrm{d}r = \int_0^\infty \frac{\varphi(r,t)}{t_\mathrm{r}} \left\{ 2\sigma n(r,t)\, l - 2\sigma_{\mathrm{gsa}} n_{\mathrm{sg}}(r,t)\, l_\mathrm{s} - 2\sigma_{\mathrm{esa}} \left[ n_{\mathrm{s0}} - n_{\mathrm{sg}}(r,t) \right] l_\mathrm{s} - \ln(1/R) - L \right\} 2\pi r\,\mathrm{d}r\,, \tag{1}$$

$$\frac{\mathrm{d}n(r,t)}{\mathrm{d}t} = -\gamma\sigma c\varphi(r,t)\, n(r,t)\,, \tag{2}$$

$$\frac{\mathrm{d}n_{\mathrm{sg}}(r,t)}{\mathrm{d}t} = -\frac{S_\mathrm{g}}{S_\mathrm{s}} \sigma_{\mathrm{gsa}} c\varphi(r,t)\, n_{\mathrm{sg}}(r,t)\,, \tag{3}$$

where $\varphi(r,t)$ is the intracavity photon density at the position of the gain medium and $n(r,t)$ is the population-inversion density; $n_{\mathrm{sg}}(r,t)$ and $n_{\mathrm{s0}}$ are, respectively, the ground-state and total population densities of the saturable absorber; $\sigma$ and

✉ Fax: +86-531-88364613, E-mail: xyz@sdu.edu.cn

$l$ are, respectively, the stimulated-emission cross section and length of the gain medium; $\sigma_{\mathrm{gsa}}$ and $\sigma_{\mathrm{esa}}$ are, respectively, the ground-state and excited-state cross sections of the saturable absorber; $l_{\mathrm{s}}$ is the length of the saturable absorber; $t$ is time; $t_{\mathrm{r}} = 2l/c$ is the round-trip transit time of light in the resonator of optical length $l'$, $c$ is the light speed in vacuum, $R$ is the reflectivity of the output mirror, $L$ is the remaining round-trip dissipative optical loss; $S_{\mathrm{g}}$ and $S_{\mathrm{s}}$ are, respectively, the beam cross-section areas in the gain medium and in the saturable absorber; and $\gamma$ is the net reduction in the population inversion resulting from the stimulated emission of a single photon. In (1)–(3) the pumping and the spontaneous emission during the pulse formation are neglected. Since most solid-state saturable absorbers are of slow recovery, the ground-state recovery of the saturable absorber during the formation of the Q-switched pulse is also neglected.

Considering the $\mathrm{TEM}_{00}$ laser mode, the intracavity photon density $\varphi(r, t)$ can be expressed as

$$\varphi(r, t) = \varphi(0, t) \exp\left(-\frac{r^2}{\omega_{\mathrm{LI}}^2}\right) , \tag{4}$$

where $\omega_{\mathrm{LI}} = (\sqrt{2}/2)\omega_{\mathrm{L}}$, $\omega_{\mathrm{L}}$ is the average radius of the intracavity laser beam in the gain medium and $\varphi(0, t)$ is the intracavity photon density on the laser axis.

When the pump beam is supposed to have a top-hat distribution, the initial population-inversion density $n(r, 0)$ can be expressed as

$$n\,(r, 0) = n_1\,(0, 0)\,\Theta\,(r - \omega_{\mathrm{PI}}) \ , \quad \Theta\,(x) = \begin{cases} 1 & (x \le 0)\,, \\ 0 & (x \ge 0)\,, \end{cases} \tag{5}$$

where $\omega_{\mathrm{PI}}$ is the average pump beam radius in the gain medium under a top-hat pump beam distribution and $n_1(0, 0)$ is the initial population-inversion density on the laser axis.

Substituting (4) and (5) into (2), we obtain

$$n\,(r, t) = n_1\,(0, 0)\,\Theta\,(r - \omega_{\mathrm{PI}}) \times \exp\left[-\gamma\sigma c \int_0^t \varphi(0, t)\,\mathrm{d}t \exp\left(-\frac{r^2}{\omega_{\mathrm{LI}}^2}\right)\right] . \tag{6}$$

The initial saturable absorber ground state population density is

$$n_{\mathrm{sg}}\,(r, 0) = n_{\mathrm{s0}}\,. \tag{7}$$

Substituting (7) and (4) into (3), we obtain

$$n_{\mathrm{sg}}\,(r, t) = n_{\mathrm{s0}} \exp\left[-\frac{S_{\mathrm{g}}}{S_{\mathrm{s}}}\sigma_{\mathrm{gsa}} c \int_0^t \varphi\,(0, t)\ \mathrm{d}t \exp\left(-\frac{r^2}{\omega_{\mathrm{LI}}^2}\right)\right] . \tag{8}$$

Substituting (4), (6), and (8) into (1), we obtain

$$\frac{\mathrm{d}\varphi(0, t)}{\mathrm{d}t} = \frac{2\sigma l}{t_{\mathrm{r}}}\varphi(0, t) n_1(0, 0) \times \frac{\exp\left[-\gamma\sigma c \int_0^t \varphi(0, t)\,\mathrm{d}t \exp\left(-\frac{\omega_{\mathrm{PI}}^2}{\omega_{\mathrm{LI}}^2}\right)\right] - \exp\left[-\gamma\sigma c \int_0^t \varphi(0, t)\,\mathrm{d}t\right]}{\gamma\sigma c \int_0^t \varphi(0, t)\,\mathrm{d}t} - \frac{2\left(\sigma_{\mathrm{gsa}} - \sigma_{\mathrm{esa}}\right) l_{\mathrm{s}}}{t_{\mathrm{r}}}\varphi\,(0, t)\, n_{\mathrm{s0}} \times \frac{1 - \exp\left[-\frac{S_{\mathrm{g}}}{S_{\mathrm{s}}}\sigma_{\mathrm{gsa}} c \int_0^t \varphi(0, t)\,\mathrm{d}t\right]}{\frac{S_{\mathrm{g}}}{S_{\mathrm{s}}}\sigma_{\mathrm{gsa}} c \int_0^t \varphi(0, t)\,\mathrm{d}t} - \frac{\varphi(0, t)}{t_{\mathrm{r}}}\left[\ln\left(\frac{1}{R}\right) + \frac{\sigma_{\mathrm{esa}}}{\sigma_{\mathrm{gsa}}}\ln\left(\frac{1}{T_0^2}\right) + L\right] . \tag{9}$$

By using $t = 0$ and $\mathrm{d}\varphi(0, t)/\mathrm{d}t = 0$, we can obtain the initial population-inversion density on the laser axis:

$$n_1(0, 0) = \frac{\ln\left(\frac{1}{R}\right) + \ln\left(\frac{1}{T_0^2}\right) + L}{2\sigma l\left[1 - \exp\left(-\frac{\omega_{\mathrm{PI}}^2}{\omega_{\mathrm{LI}}^2}\right)\right]} . \tag{10}$$

Substituting (10) into (9), and introducing some normalized parameters, we can obtain the normalized rate equation under a top-hat pump beam distribution:

$$\frac{\mathrm{d}\Phi(0, \tau)}{\mathrm{d}\tau} = \Phi(0, \tau)\frac{\exp\left[-A\,(\tau)\exp\left(-\frac{\omega_{\mathrm{PI}}^2}{\omega_{\mathrm{LI}}^2}\right)\right] - \exp\left[-A(\tau)\right]}{A\,(\tau)\left[1 - \exp\left(-\frac{\omega_{\mathrm{PI}}^2}{\omega_{\mathrm{LI}}^2}\right)\right]} - \left(1 - \frac{1}{N}\right)\Phi(0, \tau)\frac{1 - \exp\left[-\alpha A(\tau)\right]}{\alpha A(\tau)} - \frac{\Phi(0, \tau)}{N} , \tag{11}$$

where $\Phi(0, \tau)$ is the normalized photon intensity on the laser axis, $\tau$ is normalized time, $\alpha$ is a parameter indicating how easily the saturable absorber can be bleached; the larger $\alpha$, the more easily the saturable absorber can be bleached [18–21]; and $\tau$, $\alpha$, $N$, $\Phi(0, \tau)$, and $A(\tau)$ can be written as

$$\tau = \frac{t}{t_{\mathrm{r}}}\left[\ln\left(\frac{1}{R}\right) + \ln\left(\frac{1}{T_0^2}\right) + L\right] , \tag{12}$$

$$\alpha = \frac{\sigma_{\mathrm{gsa}} S_{\mathrm{g}}}{\gamma\sigma S_{\mathrm{s}}} , \tag{13}$$

$$N = \frac{\ln\left(\frac{1}{R}\right) + \ln\left(\frac{1}{T_0^2}\right) + L}{\ln\left(\frac{1}{R}\right) + \left(\frac{\sigma_{\mathrm{esa}}}{\sigma_{\mathrm{gsa}}}\right)\ln\left(\frac{1}{T_0^2}\right) + L} , \tag{14}$$

$$\Phi(0, \tau) = \varphi(0, \tau)\frac{\gamma\sigma c t_{\mathrm{r}}}{\ln\left(\frac{1}{R}\right) + \ln\left(\frac{1}{T_0^2}\right) + L} , \tag{15}$$

$$A(\tau) = \int_0^\tau \Phi(0, \tau)\,\mathrm{d}\tau\,. \tag{16}$$

When $\alpha$ approaches infinity, once the laser action begins, all the ground-state population will be excited to the first excited state (which we can see from (8) by setting $\sigma_{gsa} \to \infty$, which corresponds to $\alpha \to \infty$). Owing to the excited-state absorption, the transmission of the saturable absorber will be

$$T_b = \exp(-\sigma_{esa} n_{s0} l_s) = T_0^{\sigma_{esa}/\sigma_{gsa}}, \tag{17}$$

and the threshold population-inversion density on the laser axis will be

$$n_{th}(0,t) = \frac{\ln\left(\frac{1}{R}\right) + \left(\frac{\sigma_{esa}}{\sigma_{gsa}}\right)\ln\left(\frac{1}{T_0^2}\right) + L}{2\sigma l\left[1 - \exp\left(-\frac{\omega_{PI}^2}{\omega_{LI}^2}\right)\right]}. \tag{18}$$

From (10), (14), and (18) it can be seen that $N$ is the ratio of the initial population-inversion density to the threshold population-inversion density in the case of $\alpha \to \infty$.

We can conclude from (11)–(16) that the solutions of (11) depend on three composite parameters: $\alpha$, $N$, and $\omega_{PI}/\omega_{LI}$. Numerically solving (11), we can obtain a group of lines describing the laser pulse characteristics varying with these three parameters. The pulse energy $E$, pulse peak power $P_m$, and pulse width $W$ can be written as

$$E = \frac{\pi\omega_L^2 h\nu}{4\sigma\gamma}\ln\left(\frac{1}{R}\right)\Phi_{integ} = \frac{\pi\omega_L^2 h\nu}{4\sigma\gamma}\ln\left(\frac{1}{R}\right)\int_0^\infty \Phi(0,\tau)\,d\tau, \tag{19}$$

$$P_m = \frac{\pi\omega_L^2 h\nu}{4\sigma\gamma t_r}\left[\ln\left(\frac{1}{R}\right) + \ln\left(\frac{1}{T_0^2}\right) + L\right]\ln\left(\frac{1}{R}\right)\Phi_m, \tag{20}$$

$$W = \frac{\Delta\tau t_r}{\ln\left(\frac{1}{R}\right) + \ln\left(\frac{1}{T_0^2}\right) + L}, \tag{21}$$

where $h\nu$ is the photon energy, $\Delta\tau$ is the width of $\Phi(0,\tau)$ (FWHM), and $\Phi_m$ is the maximum value of $\Phi(0,\tau)$.

In [21], the initial population-inversion density was supposed to be a Gaussian distribution, and $n(r,0)$ was written as

$$n(r,0) = n_2(0,0)\exp\left(-\frac{r^2}{\omega_{PI}^2}\right), \tag{22}$$

where $\omega_{PI} = (\sqrt{2}/2)\omega_P$, $\omega_P$ is the average radius of the pump beam in the gain medium under a Gaussian pump beam distribution. The normalized rate equation obtained under a Gaussian pump beam distribution by Zhang et al. [21] was written as

$$\frac{d\Phi(0,\tau)}{d\tau} = \Phi(0,\tau)\int_0^1 \exp\left[-A(\tau)y^\beta\right]dy - \left(1 - \frac{1}{N}\right) \times \Phi(0,\tau)\frac{1-\exp[-\alpha A(\tau)]}{\alpha A(\tau)} - \frac{\Phi(0,\tau)}{N}, \tag{23}$$

where $\beta$ is a parameter associated with the ratio of the pump beam radius to the intracavity beam radius; $y$ is only a transition parameter, and will disappear during numerically solving the equation

$$\beta = \frac{1}{1 + (\omega_{LI}/\omega_{PI})^2}. \tag{24}$$

The initial population-inversion density on the laser axis was written as

$$n_2(0,0) = \frac{\ln\left(\frac{1}{R}\right) + \ln\left(\frac{1}{T_0^2}\right) + L}{2\sigma l}\left(1 + \frac{\omega_{LI}^2}{\omega_{PI}^2}\right). \tag{25}$$

Equations (19)–(21) can also be used to estimate the pulse energy, peak power, and pulse width when both the pump beam and the intracavity photon density are Gaussian distributions.

Under the plane-wave approximation, the pump beam and the intracavity beam are assumed to be uniform on the laser cross section:

$$\varphi(r,t) = \varphi(0,t), \tag{26}$$

$$n(r,0) = n_3(0,0). \tag{27}$$

Using the same normalizing process, we can obtain the normalized rate equation under the plane-wave approximation:

$$\frac{d\Phi}{d\tau} = \Phi\exp[-A(\tau)] - \left(1 - \frac{1}{N}\right)\Phi\exp[-\alpha A(\tau)] - \frac{\Phi}{N}. \tag{28}$$

The initial population-inversion density under the plane-wave approximation is

$$n_3(0,0) = \frac{\ln\left(\frac{1}{R}\right) + \ln\left(\frac{1}{T_0^2}\right) + L}{2\sigma l}. \tag{29}$$

## 3 Solution of equations

Equation (11) is the normalized rate equation under a top-hat pump beam distribution. The solutions of (11) depend on three composite parameters: $\alpha$, $N$, and $\omega_{PI}/\omega_{LI}$. Equation (23) is the normalized rate equation under a Gaussian pump beam distribution. The solutions of (23) also depend on three composite parameters: $\alpha$, $N$, and $\omega_{PI}/\omega_{LI}$. Equation (28) is the normalized rate equation under the plane-wave approximation. The solutions of (28) depend on only two composite parameters: $\alpha$ and $N$. The plane-wave approximation method cannot reflect the influence caused by the variation of $\omega_{PI}/\omega_{LI}$.

Figures 1 and 2 show the variation of $\Phi_{integ}$ and $\Delta\tau$ with $\omega_{PI}/\omega_{LI}$ for a Gaussian pump beam distribution and a plane-wave approximation, respectively. Under a Gaussian pump beam distribution, $\Phi_{integ}$ increases with increasing $\omega_{PI}/\omega_{LI}$ while $\Delta\tau$ decreases with increasing $\omega_{PI}/\omega_{LI}$. Under the plane-wave approximation, $\Phi_{integ}$ and $\Delta\tau$ are independent of $\omega_{PI}/\omega_{LI}$. We can easily see the big difference between the results under a Gaussian pump beam distribution and those under the plane-wave approximation.

The difference between (11) and (23) is reflected by the first term. This difference varies with the variation of $\omega_{PI}/\omega_{LI}$. When $\omega_{PI} \gg \omega_{LI}$ and $\omega_{PI} \ll \omega_{LI}$, the difference disappears. Equations (11) and (23) can be converted to the same equation when $\omega_{PI} \gg \omega_{LI}$ and $\omega_{PI} \ll \omega_{LI}$:

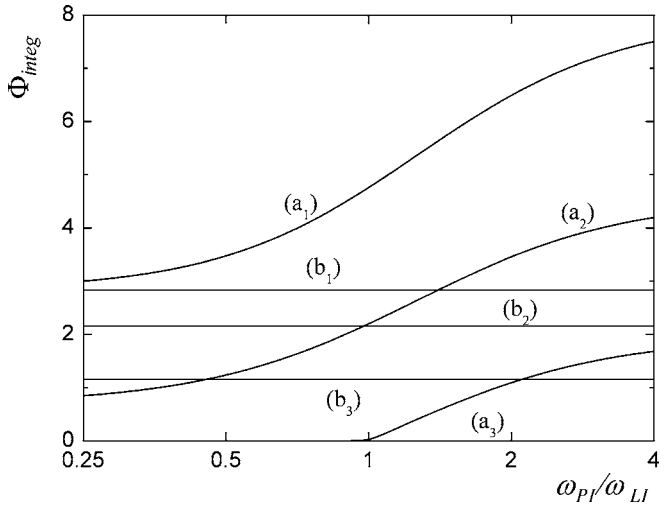


**FIGURE 1** Relation between $\Phi_{\text{integ}}$ and $\omega_{\text{PI}}/\omega_{\text{LI}}$ for different $\alpha$ in the case of $N = 3$, under Gaussian pump beam distribution: ($a_1$) $\alpha \to \infty$, ($a_2$) $\alpha = 4$, ($a_3$) $\alpha = 2$; under plane-wave approximation: ($b_1$) $\alpha \to \infty$, ($b_2$) $\alpha = 4$, ($b_3$) $\alpha = 2$

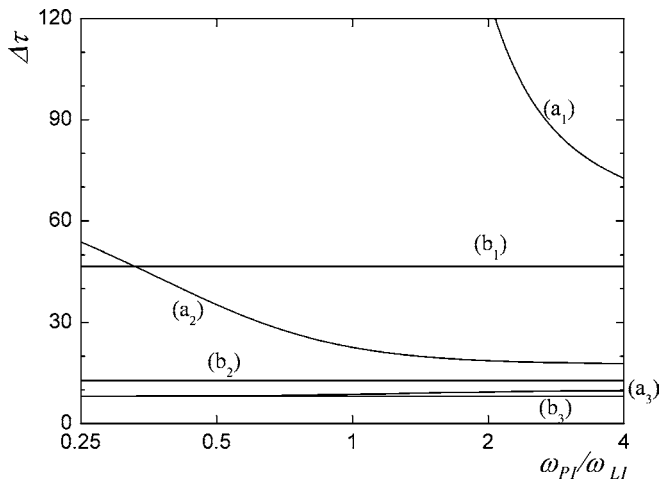


**FIGURE 2** Relation between $\Delta\tau$ and $\omega_{\text{PI}}/\omega_{\text{LI}}$ for different $\alpha$ in the case of $N = 3$, under Gaussian pump beam distribution: ($a_1$) $\alpha \to \infty$, ($a_2$) $\alpha = 4$, ($a_3$) $\alpha = 2$; under plane-wave approximation: ($b_1$) $\alpha \to \infty$, ($b_2$) $\alpha = 4$, ($b_3$) $\alpha = 2$

$$\frac{\mathrm{d}\Phi}{\mathrm{d}\tau} = \Phi\frac{1-\exp[-A(\tau)]}{A(\tau)} - \left(1-\frac{1}{N}\right)\Phi\frac{1-\exp[-\alpha A(\tau)]}{\alpha A(\tau)} - \frac{\Phi}{N}, \quad \omega_{\text{PI}} \gg \omega_{\text{LI}}, \tag{30}$$

$$\frac{\mathrm{d}\Phi}{\mathrm{d}\tau} = \Phi\exp[-A(\tau)] - \left(1-\frac{1}{N}\right)\Phi\frac{1-\exp[-\alpha A(\tau)]}{\alpha A(\tau)} - \frac{\Phi}{N}, \quad \omega_{\text{PI}} \ll \omega_{\text{LI}}. \tag{31}$$

When $\omega_{\text{PI}} \gg \omega_{\text{LI}}$, the initial population-inversion density becomes uniform in the gain medium under both Gaussian and top-hat distributions. $\omega_{\text{PI}} \gg \omega_{\text{LI}}$ represents the situation of flashlamp-pumped or laser diode side-pumped lasers. When $\omega_{\text{PI}} \ll \omega_{\text{LI}}$, the pump beam is near a line along the laser axis, which does not exist in reality. For a laser diode end-pumped laser, if $\omega_{\text{PI}} \ll \omega_{\text{LI}}$, the thermal effect will be serious, which should be avoided. So, we will not discuss the situation of $\omega_{\text{PI}} \ll \omega_{\text{LI}}$ in this paper.

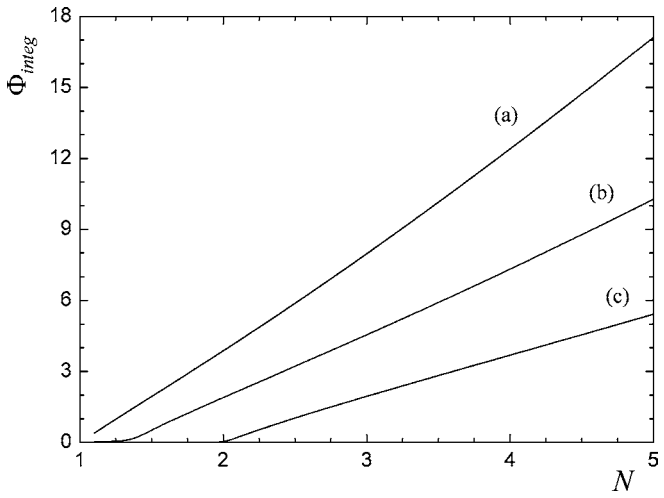


**FIGURE 3** Relation between $\Phi_{\text{integ}}$ and $N$ for different $\alpha$ in the case of $\omega_{\text{PI}} \gg \omega_{\text{LI}}$, under top-hat pump beam distribution and Gaussian pump beam distribution: (a) $\alpha \to \infty$, (b) $\alpha = 4$, (c) $\alpha = 2$

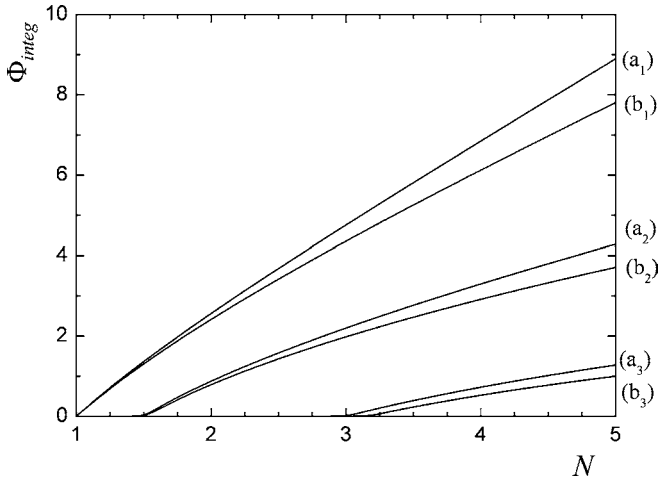


**FIGURE 4** Relation between $\Phi_{\text{integ}}$ and $N$ for different $\alpha$ in the case of $\omega_{\text{PI}} = \omega_{\text{LI}}$, under Gaussian pump beam distribution: ($a_1$) $\alpha \to \infty$, ($a_2$) $\alpha = 4$, ($a_3$) $\alpha = 2$; under top-hat pump beam distribution: ($b_1$) $\alpha \to \infty$, ($b_2$) $\alpha = 4$, ($b_3$) $\alpha = 2$

When $\omega_{\text{PI}}$ and $\omega_{\text{LI}}$ are comparable, the two pump beam distributions exhibit different influences on the laser pulse characteristics. When $\omega_{\text{PI}} = \omega_{\text{LI}}$, (11) and (23) can be converted into the following equations (32) and (33), respectively:

$$\frac{\mathrm{d}\Phi}{\mathrm{d}\tau} = \Phi\frac{\exp\left[-A(\tau)\exp(-1)\right] - \exp[-A(\tau)]}{A(\tau)\left[1-\exp(-1)\right]} - \left(1-\frac{1}{N}\right)\Phi\frac{1-\exp[-\alpha A(\tau)]}{\alpha A(\tau)} - \frac{\Phi}{N}, \quad \text{top-hat}, \tag{32}$$

$$\frac{\mathrm{d}\Phi}{\mathrm{d}\tau} = \Phi\frac{2}{A(\tau)}\left\{\frac{1-\exp[-A(\tau)]}{A(\tau)} - \exp[-A(\tau)]\right\} - \left(1-\frac{1}{N}\right)\Phi\frac{1-\exp[-\alpha A(\tau)]}{\alpha A(\tau)} - \frac{\Phi}{N}, \quad \text{Gaussian}. \tag{33}$$

Figures 3 and 4 show the relations between $\Phi_{\text{integ}}$ and $N$ for different $\alpha$ in the cases of $\omega_{\text{PI}} \gg \omega_{\text{LI}}$ and $\omega_{\text{PI}} = \omega_{\text{LI}}$ under top-hat and Gaussian pump beam distributions, respectively.

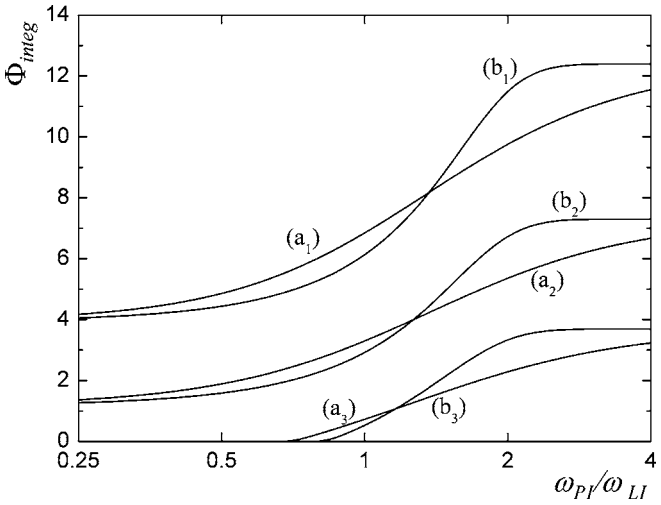


**FIGURE 5** Relation between $\Phi_{\text{integ}}$ and $\omega_{\text{PI}}/\omega_{\text{LI}}$ for different $\alpha$ in the case of $N = 4$, under Gaussian pump beam distribution: ($a_1$) $\alpha \to \infty$, ($a_2$) $\alpha = 4$, ($a_3$) $\alpha = 2$; under top-hat pump beam distribution: ($b_1$) $\alpha \to \infty$, ($b_2$) $\alpha = 4$, ($b_3$) $\alpha = 2$

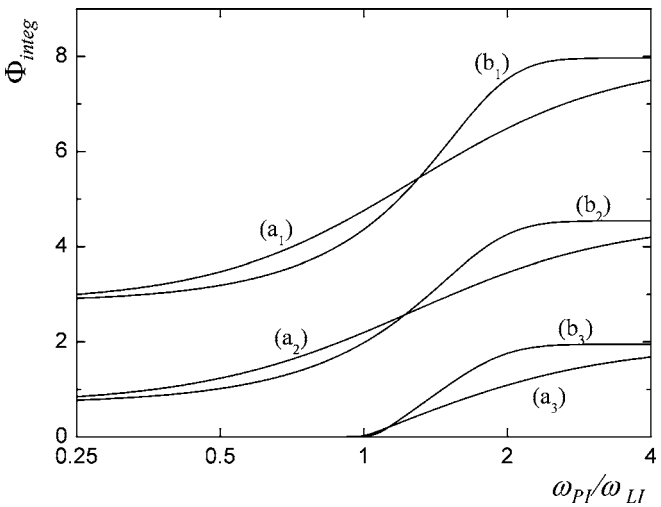


**FIGURE 6** Same as Fig. 5 except for $N = 3$

Figures 5–7 show the relations between $\Phi_{\text{integ}}$ and $\omega_{\text{PI}}/\omega_{\text{LI}}$ for different $\alpha$ under top-hat and Gaussian pump beam distributions in the cases of $N = 4$, 3, and 2, respectively. It can be seen that, for given $N$ and $\alpha$, $\Phi_{\text{integ}}$ for a top-hat distribution is smaller than that for a Gaussian distribution when $\omega_{\text{PI}}/\omega_{\text{LI}}$ is relatively small. When $\omega_{\text{PI}}/\omega_{\text{LI}}$ is relatively large, $\Phi_{\text{integ}}$ for a top-hat distribution is larger than that for a Gaussian distribution. However, the differences between the values of $\Phi_{\text{integ}}$ for the two pump beam spatial distributions are much smaller than the differences between the values of $\Phi_{\text{integ}}$ under a top-hat pump beam distribution and those under the plane-wave approximation.

Figures 8 and 9 show the variation of $\Delta\tau$ with $N$ for different $\alpha$ in the cases of $\omega_{\text{PI}} \gg \omega_{\text{L}}$ and $\omega_{\text{PI}} = \omega_{\text{LI}}$, respectively. Figures 10–12 show the variation of $\Delta\tau$ with $\omega_{\text{PI}}/\omega_{\text{LI}}$ for different $\alpha$ in the cases of $N = 4$, 3, and 2, respectively. It can be seen that, for given $N$ and $\alpha$, $\Delta\tau$ under a top-hat distribution is smaller than that under a Gaussian distribution when $\omega_{\text{PI}}/\omega_{\text{LI}}$ is relatively small and it becomes larger when $\omega_{\text{PI}}/\omega_{\text{LI}}$ is relatively large. However, the differences between the values of

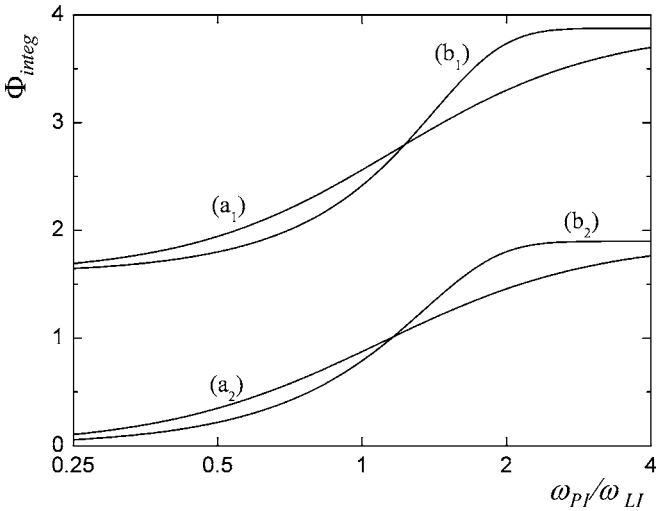


**FIGURE 7** Same as Fig. 5 except for $N = 2$. Since the Q-switching cannot be realized for $\alpha = 2$ in the case of $\omega_{\text{PI}}/\omega_{\text{LI}} < 4$ and $N = 2$, there are no curves ($a_3$) and ($b_3$) in this figure

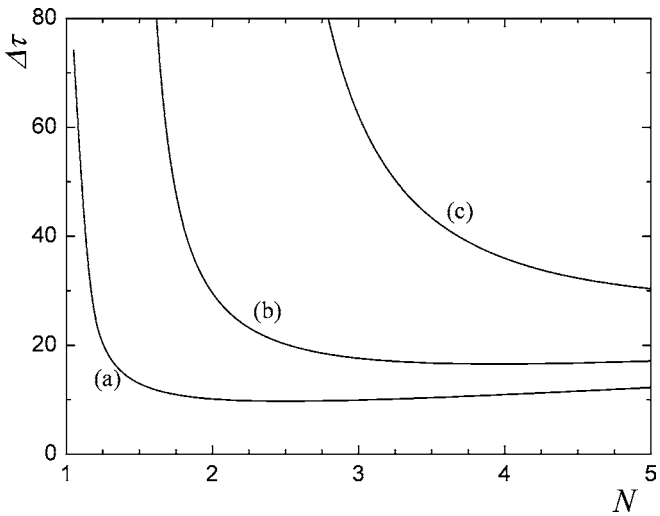


**FIGURE 8** Relation between $\Delta\tau$ and $N$ for different $\alpha$ in the case of $\omega_{\text{PI}} \gg \omega_{\text{LI}}$, under top-hat pump beam distribution and Gaussian pump beam distribution: (a) $\alpha \to \infty$, (b) $\alpha = 4$, (c) $\alpha = 2$

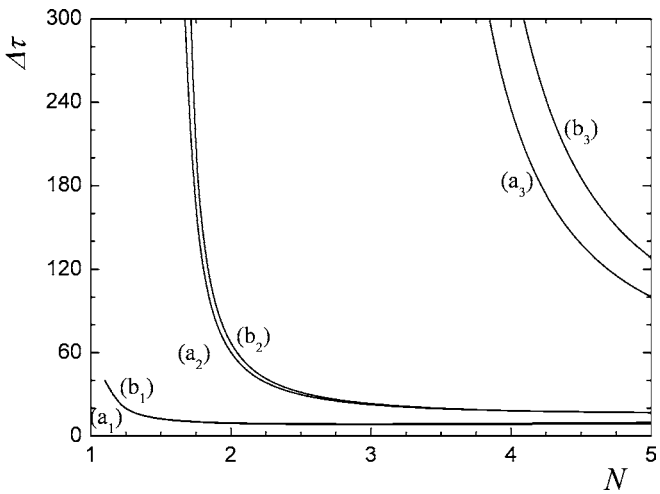


**FIGURE 9** Relation between $\Delta\tau$ and $N$ for different $\alpha$ in the case of $\omega_{\text{PI}} = \omega_{\text{LI}}$, under Gaussian pump beam distribution: ($a_1$) $\alpha \to \infty$, ($a_2$) $\alpha = 4$, ($a_3$) $\alpha = 2$; under top-hat pump beam distribution: ($b_1$) $\alpha \to \infty$, ($b_2$) $\alpha = 4$, ($b_3$) $\alpha = 2$

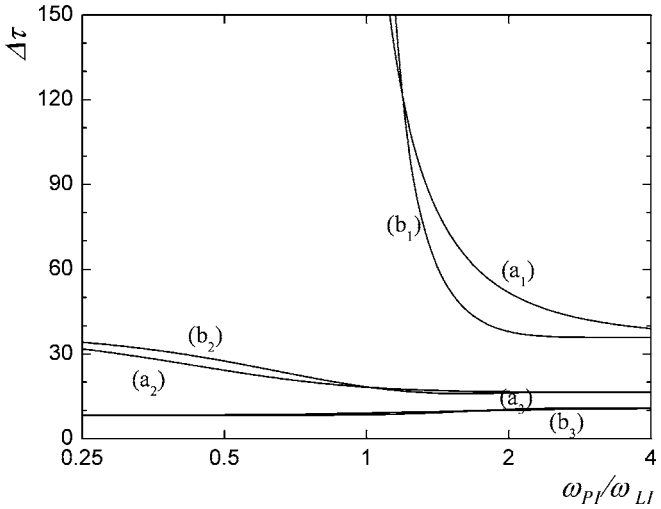


**FIGURE 10** Relation between $\Delta\tau$ and $\omega_{\rm PI}/\omega_{\rm LI}$ for different $\alpha$ in the case of $N = 4$, under Gaussian pump beam distribution: $(a_1)\ \alpha \to \infty$, $(a_2)\ \alpha = 4$, $(a_3)\ \alpha = 2$; under top-hat pump beam distribution: $(b_1)\ \alpha \to \infty$, $(b_2)\ \alpha = 4$, $(b_3)\ \alpha = 2$

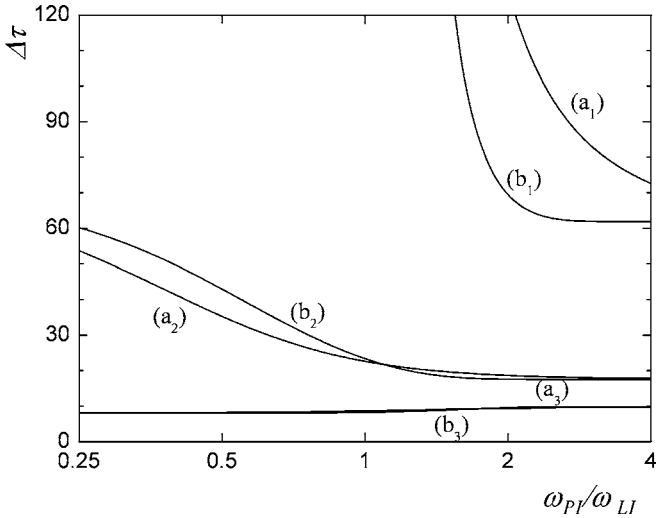


**FIGURE 11** Same as Fig. 10 except for $N = 3$

$\Delta\tau$ for the two pump beam spatial distributions are much smaller than the differences between the values of $\Delta\tau$ under a top-hat pump beam distribution and those under the plane-wave approximation.

## 4 Conclusion

We have obtained the normalized rate equations for passively Q-switched lasers under a top-hat pump beam distribution, a Gaussian pump beam distribution, and the plane-wave approximation. These normalized rate equations have been solved numerically and a group of general curves have been generated. The results show that the solutions of the rate equations under a top-hat pump beam distribution have a difference from those under a Gaussian pump beam distribution, but the difference is very limited. The solutions of the rate equations under both situations are far from those under the plane-wave approximation. This is because the plane-wave approximation method cannot reflect the influence caused by the variation of $\omega_{\rm PI}/\omega_{\rm LI}$. The validity of considering a Gaussian pump beam distribution has been proved in [21]. We believe that the solutions of the rate equations under both top-hat and Gaussian pump beam distributions can give much more precise theoretical results than those under the plane-wave approximation.

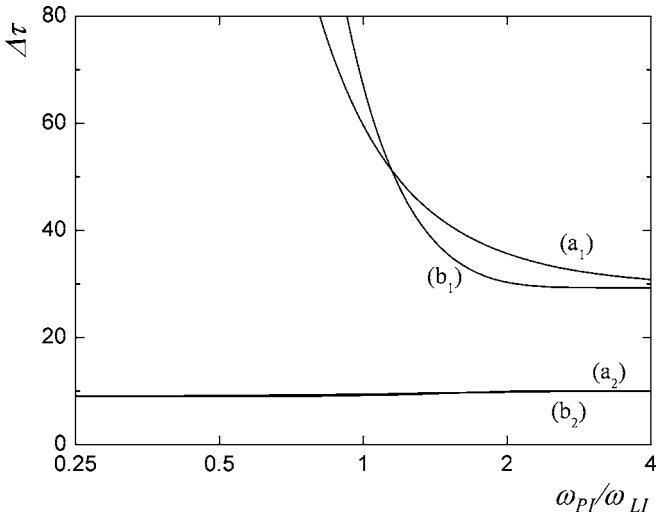


**FIGURE 12** Same as Fig. 10 except for $N = 2$. Since the Q-switching cannot be realized for $\alpha = 2$ in the case of $\omega_{\rm PI}/\omega_{\rm LI} < 4$ and $N = 2$, there are no curves $(a_3)$ and $(b_3)$ in this figure

**ACKNOWLEDGEMENTS** This work was supported by the National Natural Science Foundation of China under Grant No. 60478017, in part by the Science and Technology Development Program of Shandong Province under Grant No. 03BS095, and in part by the project sponsored by the Scientific Research Foundation for the Returned Overseas Chinese Scholars, State Education Ministry.

## REFERENCES

1 G. Wagner, B.A. Lengyel, J. Appl. Phys. **34**, 2040 (1963)
2 R.G. Kay, G.S. Waldman, J. Appl. Phys. **36**, 1319 (1965)
3 M. Michon, J. Ernest, J. Hanus, R. Auffret, Phys. Lett. **19**, 219 (1965)
4 P.C. Magnante, IEEE J. Quantum Electron. **QE-8**, 440 (1972)
5 I.B. Vitrishchak, L.N. Soms, Sov. J. Quantum Electron. **5**, 1265 (1975)
6 T.Y. Fan, IEEE J. Quantum Electron. **QE-24**, 2345 (1988)
7 J.J. Degnan, IEEE J. Quantum Electron. **QE-34**, 887 (1998)
8 J.J. Degnan, IEEE J. Quantum Electron. **QE-25**, 214 (1989)
9 J.J. Zayhowski, P.L. Kelley, IEEE J. Quantum Electron. **QE-27**, 2220 (1991)
10 X. Zhang, S. Zhao, Q. Wang, B. Ozygus, H. Weber, IEEE J. Quantum Electron. **QE-35**, 1912 (1999)
11 A. Szabo, R.A. Stein, J. Appl. Phys. **36**, 1562 (1965)
12 L.E. Erickson, A. Szabo, J. Appl. Phys. **37**, 4953 (1966)
13 L.E. Erickson, A. Szabo, J. Appl. Phys. **38**, 2540 (1967)
14 A.E. Siegman, *Lasers* (University Science Books, Mill Valley, CA, 1986), pp. 1024–1026
15 X. Zhang, S. Zhao, Q. Wang, Y. Liu, J. Wang, IEEE J. Quantum Electron. **QE-30**, 905 (1994)
16 Y.K. Kuo, M.F. Huang, M. Birnbaum, IEEE J. Quantum Electron. **QE-31**, 657 (1995)
17 T. Dascalu, G. Philipps, H. Weber, Opt. Laser Technol. **29**, 145 (1997)
18 J.J. Degnan, IEEE J. Quantum Electron. **QE-31**, 1890 (1995)
19 G. Xiao, M. Bass, IEEE J. Quantum Electron. **QE-33**, 41 (1997)
20 X. Zhang, S. Zhao, Q. Wang, Q. Zhang, L. Sun, S. Zhang, IEEE J. Quantum Electron. **QE-33**, 2286 (1997)
21 X. Zhang, S. Zhao, Q. Wang, B. Ozygus, H. Weber, J. Opt. Soc. Am. B **17**, 1166 (2000)
22 C. Ren, X. Zhang, Q. Wang, S. Zhao, J. Optoelectron. Lasers **13**, 294 (2002)